Online Near-Infrared Measurements of an Epoxy Cure Process Compared to Mathematical Modeling Based on Differential Scanning Calorimetry Measurements

H.-H. Friis-Pedersen, L. P. Houmøller, B. K. Storm

Esbjerg Technical Institute, Aalborg University, Niels Bohrs Vej 8, 6700 Esbjerg, Denmark

Received 26 January 2007; accepted 12 March 2008
DOI 10.1002/app.28407
Published online 11 August 2008 in Wiley InterScience (www.interscience.wiley.com).

ABSTRACT: An epoxy resin containing diglycidyl ether of bisphenol A, dicyandiamide, and an accelerator (diurone) was investigated under different cure cycles. The mathematical prediction of the degree of cure in a thermoset as a function of time and temperature was investigated and compared to measured data. Near-infrared analysis was used to measure the conversion of epoxy and primary amine and the production of hydroxyl. Modulated differential scanning calorimetry was used to measure the changes in the heat capacity during cure. The measurements revealed differences in the primary amine conversion and hydroxyl production, and close relations to the measurements of heat capacity were found. The measurements of the degree of cure revealed that cure cycles initiated at 80°C produced a lower degree of cure than cure cycles initiated at 90°C, although all cure cycles were postcured at 110°C. These findings were to some degree supported by measurements of the primary amine conversion and hydroxyl production. The characteristics found were attributed to differences in the cure mechanisms. The mathematical model did not incorporate these differences, and this may have led to discrepancies between the predicted and actual values of the degree of cure. © 2008 Wiley Periodicals, Inc. J Appl Polym Sci 110: 2184–2194, 2008

Key words: curing of polymers; differential scanning calorimetry (DSC); infrared spectroscopy; kinetics (polym.); thermosets

INTRODUCTION

Epoxy composite materials are often used in industry as structural components or as adhesive coatings.[1] Epoxy thermosets can be found in diverse components such as wind turbine blades, electronic components, and adhesives.

The epoxy and hardener form the basis of the mechanical and chemical properties that an epoxy thermoset attains during curing. Improving the properties usually implies changing the epoxy or hardener because the same properties of a thermoset are obtained even if it is cured under different conditions. However, for the epoxy diglycidyl ether of bisphenol A (DGEBA) and the hardener dicyandiamide (DDA) investigated in this study, different curing reactions occur at high and low temperatures, implying different mechanical properties under different curing conditions.

Many references can be found on the DGEBA–DDA resin system.[2–23] This particular epoxy system attracts considerable attention because the reaction mechanism depends on temperature, which gives different chemical and mechanical properties, as pointed out by, for instance, Amdouni et al.[23] The cure reactions primarily consist of etherification (or homopolymerization) and epoxy–amine addition reactions. The ratio of etherification (or epoxy homopolymerization) to epoxy–amine addition is the primary factor that is affected by a change in temperature.

Lin et al.,[22] Wang et al.,[17] and Amdouni et al.[23] stated that different chemical reactions occur at high and low temperatures. At low temperatures, etherification is favored because of the low solubility of DDA.[24–26] This suggests that etherification increases the brittleness and fragility of an epoxy thermoset. Etherification leads to higher glass-transition temperatures because of a combination of the copolymer effect, higher crosslinking, and a change in the functionality of the crosslinks.[22,23] Cyclization and additional primary amine addition reactions are, on the other hand, more likely to occur at higher curing temperatures. Besides etherification and amine addition reactions, different cyclization reactions can occur, complicating an exact description of the cure reactions. Detailed descriptions of the cure reaction for this complicated system can be found in refs. 2–4,18,22, and 23. In addition, Wang et al. suggested that water affects the cure reactions in such a manner that different cure products are obtained, depending on the presence of water; that is, the final epoxy network can differ, depending on the water content.

Correspondence to: B. K. Storm (bks@aaue.dk).

Typical industrial applications of the DGEBA/DDA epoxy thermoset are not aware of these issues and use cure processes covering a wide range of temperatures. To avoid overly large temperature gradients during cure caused by the strong exothermic curing reactions, the curing process of epoxy is performed with cure cycles. In this approach, some of the heat generated by the cure reactions is removed at moderate temperatures, and this prevents a strong exothermic temperature peak. After a certain period, the temperature is then increased to obtain a fully cured material. With this approach, the large temperature gradients otherwise encountered at elevated curing temperatures can be avoided. However, because of the different reaction mechanisms at high and low temperatures, different material properties may be achieved, depending on the cure cycle.

Amdouni et al.[23] investigated different cure cycles of a system consisting of DGEBA, DDA, and the catalyst benzyldimethylamine to see if these cure cycles induced any differences in mechanical properties. Interestingly, they found that Young's modulus was not affected by the different cure cycles; however, the plastic region in the stress–strain diagram was affected together with the fracture behavior. They attributed these differences to different crosslinking densities. The crosslinking density was stated to be affected by the ratio of etherification to epoxy–amine addition reactions, with etherification more likely to occur at a low temperature (100°C) because of the low solubility of DDA.

In this study, different cure cycles were investigated to obtain a deeper understanding of the cure process. The conversion of epoxy and primary amine and the production of hydroxyl were analyzed with near-infrared (NIR) analysis to investigate differences in the conversion and production ratios under different cure cycles. In addition, measurements of the degree of cure and heat capacity under quasi-isothermal conditions with differential scanning calorimetry (DSC) and modulated differential scanning calorimetry (MDSC), respectively, were performed with a similar purpose.

The cure cycles were constructed in such a way that degrees of cure of approximately 0.1, 0.2, and 0.4 were obtained in the initial temperature stage. Three cure cycles had an initial temperature of 80°C, and three other ones had an initial temperature of 90°C, for a total of six cure cycles. In all cycles, after a certain degree of cure was reached, the temperature was raised to 110°C to obtain a fully cured epoxy material.

Besides the investigation of different properties of the epoxy material, the prediction of the degree of cure under different cure cycles with a mathematical model was also addressed. The limitations of the mathematical model and the differences between the measured and predicted values were investigated.

EXPERIMENTAL

Materials

The epoxy prepreg SPX 8800 is a commercial product from SP Systems (Newport, United Kingdom); it was used as received. It is a one-formulation prepreg that contains a DGEBA-based epoxy prepolymer, a DDA hardener, and a diurone accelerator. These three components constitute approximately 45% (w/w) of the prepreg, and glass fibers (55% w/w) constructed in triaxial layers serve as the reinforcements.

Techniques

NIR analysis

A short description is given here on NIR spectroscopy; additional details may be found in Wang et al.[17]

NIR spectroscopy was performed with a Fourier transform NIR spectrometer equipped with an InAs detector (ABB Bomem, Quebec, Canada). During the cure of the epoxy prepreg, transmission spectra were recorded in the wave-number range of 3800–9000 cm^{-1} every 60 s at a resolution of 4 cm^{-1}. Each spectrum was an average of 30 scans. Before each experiment, a background spectrum was recorded as the average of 60 scans with the same experimental setup used for the samples and with similar small glass pieces. Filters were used to decrease the intensity of the transmitted light in order to not overexpose the InAs detector.

Baseline changes in the NIR spectra were found that were not correlated to any chemical changes. Accordingly, a standard normal variate transformation of each spectrum was made by subtraction of the mean absorbance, which consisted of subtraction of the mean value of each spectrum followed by division by the standard deviation of the absorbance.

The conversion of epoxy and primary amine, the production of hydroxyl, and the water desorption were calculated with the peaks designated in Table I (see also ref. 17 and references therein). As the thickness can change during the cure and the light trans-

TABLE I
Assignments of the Observed Peaks of the Chemical Groups in the Epoxy Prepreg According to Ref. 17 and References Therein

	Peak (cm^{-1})	Integration range (cm^{-1})
Epoxy group C—H	4530	4563–4502
First aromatic C—H absorption band	4600	4620–4590
Second aromatic C—H absorption band	5985	6041–5952
Primary amine N—H	5044	5067–5022
Hydroxyl O—H	7000	7101–6858

mission can also change for reasons that cannot explicitly be attributed to any chemical changes, an internal reference was needed. For the calculation of the epoxy and primary amine conversion and water desorption, the aromatic C—H absorption at 4600 cm^{-1} was used.

The aromatic C—H absorption at 5985 cm^{-1} was located more closely to the hydroxyl peak at 7000 cm^{-1} than the aromatic C—H absorption at 4600 cm^{-1}. Accordingly, the aromatic C—H absorption at 5985 cm^{-1} was used as an internal reference for the calculation of hydroxyl group production. The areas of the individual peaks were in all cases used.

This is contrary to ref. 17, in which the band heights were used for calculating the epoxy conversion and the hydroxyl group production. No significant differences were found between these two calculation methods with data from this study.

The epoxy conversion, primary amine conversion, and water desorption were calculated with eqs. (1)–(3), respectively:

$$\alpha_{\text{Epoxy}} = \left(1 - \frac{A_{\text{Epoxy},t}/A_{\text{Ref},t}}{A_{\text{Epoxy},0}/A_{\text{Ref},0}}\right) \times 100\% \quad (1)$$

$$\alpha_{A\,\text{min}\,e} = \left(1 - \frac{A_{\text{A min e},t}/A_{\text{Ref},t}}{A_{\text{A min e},0}/A_{\text{Ref},0}}\right) \times 100\% \quad (2)$$

where α_{Epoxy} is the epoxy conversion, α_{Amine} is the primary amine conversion, A is the peak area, the subscript t refers to time t, the subscript 0 refers to time 0, and the subscript Ref refers to the reference peak.

The hydroxyl production was calculated on the basis of the primary amine content at the beginning of the epoxy cure process. Any reaction between the primary amine (DDA) and DGEBA leads to the formation of a hydroxyl group. However, DDA has multifunctionality, and the literature is not clear on this. Accordingly, the functionality of DDA is not known and is set to 1.

Any decrease in the concentration of the primary amine must lead to an increase in the hydroxyl concentration. However, because the relation between the concentration and absorbance is not known, that is, the molar extinction coefficients are not known, the relation between the primary amine and hydroxyl can be only relative. Hence, the following equation was used to calculate the relative hydroxyl production:

$$\alpha_{\text{Hydroxyl}} = \left(\frac{A_{\text{OH},t}/A_{\text{Ref},t} - A_{\text{OH},0}/A_{\text{Ref},t}}{A_{\text{A min e},0}/A_{\text{Ref},0}}\right) \times 100\% \quad (3)$$

where α_{Hydroxyl} is the hydroxyl production and A_{Ref} is the area of the second aromatic C—H absorption band. The second aromatic C—H absorption band was used as a reference for the hydroxyl production calculations instead of the first aromatic C—H absorption band because the location of the second aromatic C—H absorption band peak was closer to the hydroxyl peak and was estimated to give more reliable results.

DSC

For the measurement of the heat flux generated during the cure, a Mettler–Toledo DSC (Zurich, Switzerland) 822e instrument equipped with an FRS 5 sensor and a TSO 801RO universal sample robot autosampler was used. The DSC apparatus was calibrated in terms of temperature and heat flow with an indium standard. All measurements were conducted in an air atmosphere. The sample sizes varied from 10 to 25 mg, and they were all analyzed in 40-μL aluminum pans.

For the cure cycle experiments, duplicated measurements were made to assess the reproducibility of the measured data. In all, more than 12 measurements were conducted. Data treatment was performed with Matlab 5.3 software.

As the ratio of the glass fibers to the amount of resin could vary from sample to sample because of the very small sample sizes, the amount of epoxy resin was estimated through the heating of the aluminum sample pans containing the epoxy prepreg at 600°C for 30 min. The sample pans were then weighed after cooling. The weight loss was assumed to be the amount of resin in the sample.

The degree of cure was calculated according to the following equation:[1,27–30]

$$\alpha(t') = \frac{1}{\Delta H_{\text{Total}}} \int_0^{t'} q_{Rxn}(t)dt \quad (4)$$

where $\alpha(t')$ is the degree of cure at time t', ΔH_{Total} is the total enthalpy of reaction, and $q_{Rxn}(t)$ is the heat flux measured by the DSC instrument. ΔH_{Total} was measured at 120°C as the average of five repeated experiments. ΔH_{Total} was also measured at 115°C but did not show any differences from the measurements conducted at 120°C.

At least five isothermal DSC experiments were performed at temperatures of 80, 90, 100, and 110°C to develop a mathematical model predicting the degree of cure as a function of time and temperature. In all, more than 20 experiments were performed.

Quasi-isothermal temperature modulated differential scanning calorimetry (TMDSC) measurements were made to measure the changes in the heat capacity during cure. All measurements were conducted with an amplitude of 1°C and a period of 120 s. Generally, it was found that the nonreversing

heat flux curves from MDSC measurements were more prone to baseline problems than nonmodulated DSC measurements. Accordingly, although the MDSC measurements also provided measurements of the nonreversing heat flux during cure, the heat flux curves obtained in the nonmodulated mode were used to determine the degree of cure in accordance with the aforementioned description.

Following each cure cycle, a temperature scan in the modulated mode was conducted to measure the glass-transition temperature. The TMDSC scan was conducted with an overall heating rate of 2°C/min, an amplitude of 3°C, and a period of 120 s. Each TMDSC scan was made in the range of −20 to 250°C. The glass-transition temperature was determined as the point of inflection of the modulus of the heat capacity curve.

All measurements of the heat capacity were relative because of problems with calibration; however, the changes in the heat capacity as a function of time were not affected by these problems.

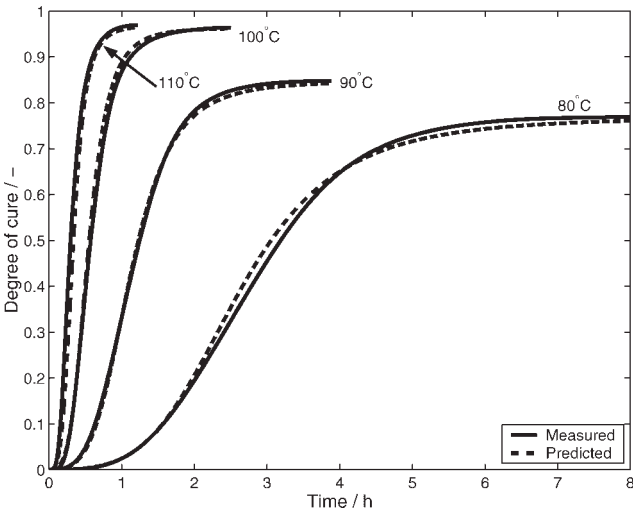

Figure 1 Isothermal degree of cure as a function of time, measured with the DSC instrument and eq. (4). The curves of the predicted degree of cure were calculated with eq. (5) with the parameters given in Table II.

RESULTS AND DISCUSSION

DSC measurements and the mathematical model

Isothermal measurements of the degree of cure at temperatures of 80, 90, 100, and 110°C are illustrated in Figure 1. Predictions of the degree of cure as a function of time and temperature are also provided in Figure 1, corresponding to solutions of eq. (5).

The mathematical model used to predict the degree of cure as a function of time and temperature is given in eq. (5):

$$\frac{d\alpha}{dt} = A \exp\left(-\frac{E_a}{RT}\right)\alpha^n(\alpha_m - \alpha)^m \qquad (5)$$

where α is the degree of cure, α_m is the final degree of cure at the current temperature, m and n are constants, A is the pre-exponential factor, E_a is the energy of activation, R is the gas constant, and T is the temperature.

Usually, n and m are constants independent of temperature; however, in a few cases, they are functions of temperature.[31]

Equation (5) was originally proposed by Sourour and Kamal.[32] Numerous references apply eq. (5) or similar equations to relate the degree of cure to the rate of cure, time, and temperature.[27,32–50]

Keenan[31] provided an elegant and relatively simple approach for fitting eq. (5) with $\alpha_m = 1$ to measured values of the curing behavior of an epoxy film adhesive.

The initial condition for solving eq. (5) is usually $\alpha = 0$ at $t = 0$, from which it is evident that $d\alpha/dt = 0$. In addition, it is immediately apparent that when $\alpha \to \alpha_m$, then $d\alpha/dt \to 0$. Accordingly, the rate of reaction is zero at the beginning of the cure process, and because the degree of cure will approach α_m at the end, it follows that the rate of cure will also approach zero.

Keenan[31] applied eq. (5) with $\alpha_m = 1$, which implies $\alpha \to 1$ for all temperatures. Usually, curing at low temperatures does not lead to a fully cured material because of vitrification (i.e., $\alpha_m < 1$); hence, using eq. (5) with $\alpha_m = 1$ will not lead to a satisfactory prediction of low-temperature cure processes at the end.

Garcia-Padron et al.[51] used eq. (5), in which α_m is the final degree of cure depending on the temperature, and Kosar and Gomzi[33] described a similar approach. For our system, $\alpha_m = 0.77$ at 80°C, $\alpha_m = 0.85$ at 90°C, $\alpha_m = 0.96$ at 100°C, and $\alpha_m = 0.97$ at 110°C. Clearly, for the system in this study, $\alpha_m \neq 1$ for cure processes at low temperatures, and this is also confirmed by the predictions obtained on the basis of eq. (5) and illustrated in Figure 1.

The approach given by Keenan[31] for finding the constants in eq. (5) was primarily based on the location of the peak value of the epoxy curing system, that is, the value of the degree of cure at which the rate of cure has its peak value, which is designated by α_p. A similar approach has been used here in combination with a refined optimization of the parameters to improve the fit to the measured values. The optimization of the parameters was performed with a nonlinear least square method (lsqcurvefit) available in Matlab. The obtained parameters are given in Table II.

A comparison with Kissinger's method[52] was not performed in this study. This work is restricted to

TABLE II
Physical Parameters Applied in Eq. (5)

Variable	Value
E_a	4491 J/mol
A	0.46 s^{-1}
n	0.776
m	1.224
R	8.31 J $mol^{-1}.^{\circ}C^{-1}$

eq. (5) because of the very good fitting characteristics given by this expression.

Keenan[31] found a temperature dependence of the constants n and m; however, the fit obtained with eq. (5) with the parameters given in Table II was found to be adequate. In other words, n and m were found to be independent of temperature.

Equation (5) cannot be solved if the initial degree of cure is equal to zero; therefore, a value of $\alpha = 0.0001$ was used. Solutions of eq. (5) are illustrated in Figure 1, in which the parameters given in Table II are applied. The Runge–Kutta fourth-order method was used to solve eq. (5), and the aforementioned values of α_m were used in the solution.

With an approach similar to that described previously, the degree of cure was predicted by eq. (5) for the six different cure cycles and compared to measured data. The data measured with DSC measurements of the heat flux and eq. (4) were used to obtain values of the degree of cure. The comparison of the measured and predicted data with solutions of eq. (5) is illustrated in Figures 2 and 3 for cure cycles initiated at 80 and 90°C, respectively.

In all cases, the measured values of the degree of cure for cycles initiated at 80°C indicated that the final degree of cure was significantly lower (the final

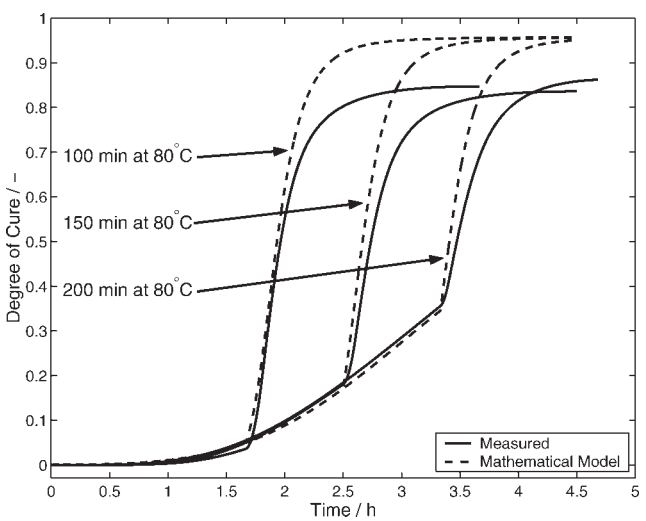

Figure 2 Degree of cure as a function of time, measured with the DSC instrument. All measurements were initiated at 80°C. The predicted degree of cure, based on eq. (5) with parameters from Table II, is also shown.

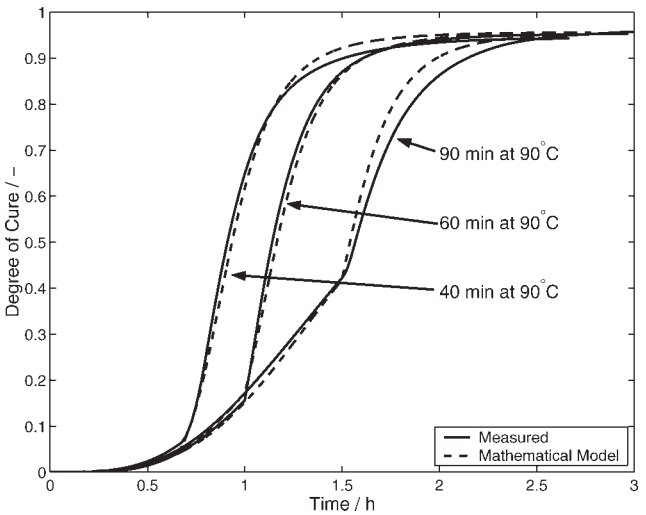

Figure 3 Degree of cure as a function of time, measured with the DSC instrument. All measurements were initiated at 90°C. The predicted degree of cure, based on eq. (5) with parameters from Table II, is also shown.

degree of cure was ca. 0.85; see Fig. 2) than what would have been expected. For isothermal measurements conducted at 110°C, the final degree of cure was found to be 0.97, as mentioned previously and illustrated in Figure 1. In other words, the cure cycle initiated at 80°C did not lead to a fully cured material in terms of DSC measurements even though the temperature was increased to 110°C. Ideally, the postcure process at 110°C should allow for an almost complete final cure of the material, and the thermoset should obtain the same degree of cure as a thermoset cured at 110°C.

An illustration of measured and predicted values of the degree of cure is illustrated in Figure 3 for cure cycles initiated at 90°C. The measured values of the degree of cure approach approximately 0.96 for this particular situation, and with the mathematical model approaching a value of the degree of cure of 0.97, the predictions of the degree of cure are very close to the measured values.

For all cycle measurements initiated at 90°C, the final degree of cure is approximately 0.96. Accordingly, cure cycle measurements initiated at 90°C seemed to give an almost fully cured material in terms of DSC measurements.

These differences are explained by different reaction mechanisms at 80 and 90°C. Because of the low solubility of DDA at low temperatures (particularly below 90°C[17]), the epoxy is more likely to participate in etherification reactions or epoxy homopolymerization rather than epoxy–amine addition reactions. The decreased accessibility of DDA at low temperatures diminishes the amounts of reactants available, explaining the lower values of the degree of cure for cycles initiating at 80°C.

The mathematical model predicting the degree of cure as a function of time and temperature, represented by eq. (5), is expected to approach a final degree of cure of 0.97 at 110°C because $\alpha_m = 0.97$ at 110°C. The discrepancies clearly shown in Figure 2 were accordingly expected and cannot as such be explained by a problem with the mathematical model. More detailed insight into the reaction kinetics would be necessary to model the different developments in the degree of cure with different cure cycles.

The poor performance of the mathematical model in the case of cure cycles initiated at 80°C is due to different reaction mechanisms that the mathematical model is not equipped to handle. A detailed analysis of the reaction kinetics would be necessary to obtain a more accurate model to predict values of the degree of cure.

Measurements of the glass-transition temperature

Values of the glass-transition temperatures for the six different temperatures cycles with MDSC scans are listed in Table III. The point of inflection at the modulus of heat capacity curve was used to find the glass-transition temperature. A similar approach was used in refs. 54 and 55.

The samples with the shortest curing time had the highest glass-transition temperature.

The differences in the glass transition can be explained by several factors. The prolonged period of curing for the temperature cycles conducted for 200 min at 80°C and 90 min at 90°C may lead to a higher degree of thermal degradation, which may explain the smaller glass-transition temperature. However, taking the relatively low temperature into consideration, we find it unlikely that thermal degradation can occur.

The differences in the glass-transition temperature may also be explained by the ratio of etherification to the epoxy–amine addition reaction. The longer the cure period is at 80 or 90°C, the more etherification there is. Although a 120-min cure period at 110°C exists for all cure cycles, the longer cure periods at 80 or 90°C decrease the epoxy available for epoxy–amine addition reactions at 110°C. Hence, the higher glass-transition temperatures for experiments conducted for a short time at 80 or 90°C (i.e., 100 min at 80°C and 40 min at 90°C) are explained by a presumably larger number of epoxy–amine addition reactions due to a higher amount of epoxy available for reactions at 110°C.

TABLE III
Glass-Transition Temperature (T_g) Values from Modulated DSC Measurements

Cure method	T_g (°C)
100 min at 80°C/120 min at 110°C	116.2/117.0
150 min at 80°C/120 min at 110°C	115.25/117.0
200 min at 80°C/120 min at 110°C	115.0/114.5
40 min at 90°C/120 min at 110°C	118.0/117.25
60 min at 90°C/120 min at 110°C	116.5/117.0
90 min at 90°C/120 min at 110°C	114.5/114.25

Two separate measurements of T_g were conducted for each cure cycle with two separate samples (separated in the table with slashes).

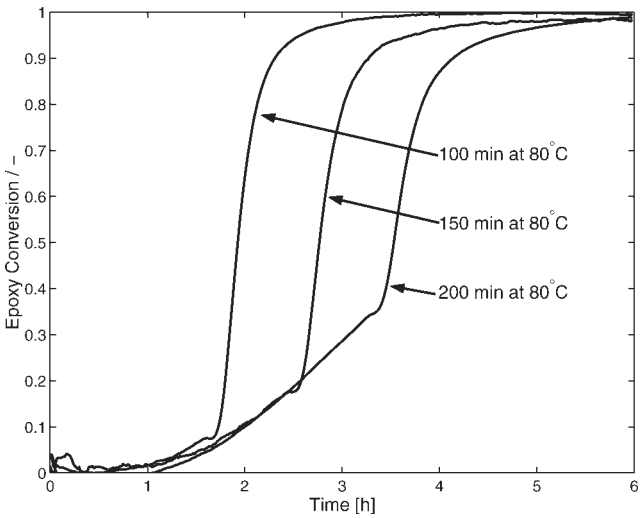

Figure 4 Conversion of epoxy initiated at 80°C as a function of time, measured with NIR analysis.

NIR analysis

The conversion of epoxy as a function of time is illustrated in Figure 4 for cure cycles initiating at 80°C and in Figure 5 for cure cycles initiating at 90°C.

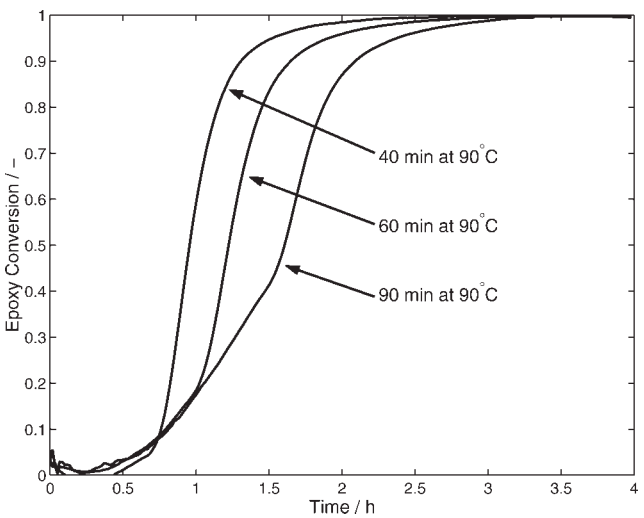

Figure 5 Conversion of epoxy initiated at 90°C as a function of time, measured with NIR analysis.

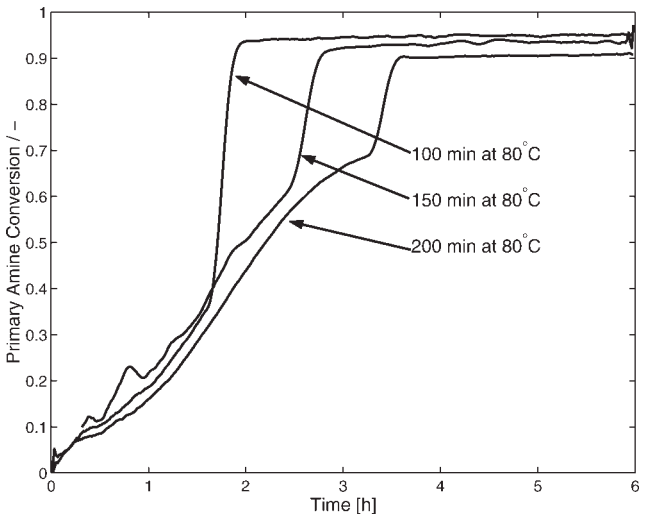

Figure 6 Conversion of primary amine initiated at 80°C as a function of time, measured with NIR analysis.

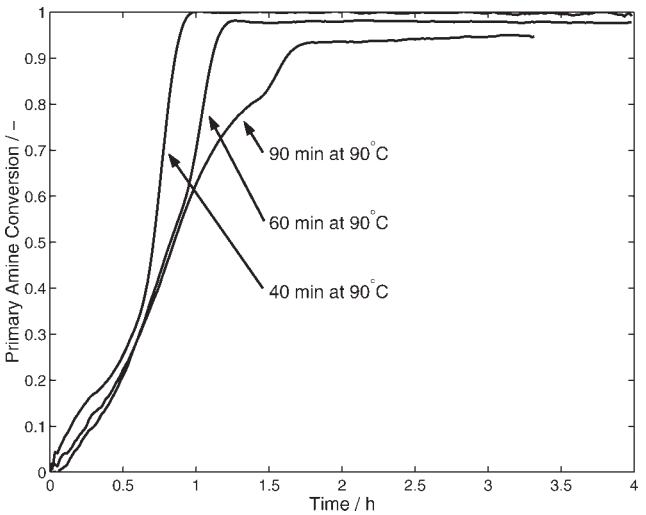

Figure 7 Conversion of primary amine initiated at 90°C as a function of time, measured with NIR analysis.

Figures 4 and 5 indicate the same development in the epoxy conversion, that is, the longer the cure at low temperatures, the higher the epoxy conversion. In none of the cases did the epoxy conversion become larger than 45% at low temperatures. The conversion of epoxy reached approximately 0.98 for the two cure cycles of 150 and 200 min at 80°C (Fig. 4) but reached 1.0 for all cure cycles initiated at 90°C (Fig. 5) and for the cure cycle of 100 min at 80°C (Fig. 4). Because of the uncertainty in the NIR quantification of functional groups, the experiment was duplicated, and a final epoxy conversion of 0.98 was confirmed for the cases of 150 and 200 min at 80°C.

The conversion of primary amine as a function of time is illustrated in Figure 6 for cure cycles initiating at 80°C and in Figure 7 for cure cycles initiating at 90°C.

Curing for 40 min at a temperature of 90°C gave the highest primary amine conversion (ca. 1.0; Fig. 7), whereas 200 min at 80°C gave the lowest conversion (ca. 0.90; Fig. 6). Ideally, a postcure treatment should erase the influence of the precure treatment, and this has generally been found to be true for other epoxy–amine systems;[23] however, because of different chemical reactions at different temperatures, this is evidently not the case for this system. In other words, the differences in the conversion of the primary amine point to the fact that the properties of the epoxy thermoset may be different, depending on the cure cycle.

As the epoxy–amine addition reaction generates hydroxyl groups, a strong correlation between the conversion of the epoxy and primary amine and the production of hydroxyl must be expected. Generally, the higher the primary amine conversion was, the higher the hydroxyl production was, as shown in Figures 6–9. For instance, the primary amine conversions for a cure cycle of 40 and 90 min at 90°C were approximately 1 and 0.95, respectively, and the hydroxyl production was approximately 0.58 and 0.49, respectively.

The hydroxyl production was approximately in the range of 0.5–0.6 for a temperature of 90°C but was in the range of approximately 0.6–0.7 for a temperature of 80°C. This was in contrast to the primary amine conversion, which was largest at 90°C.

This effect can be explained by a shift in the reaction mechanisms at 80°C, at which the epoxy is more prone to proceed under secondary amine addition rather than primary amine addition. This would lead to a continued conversion of epoxy and produc-

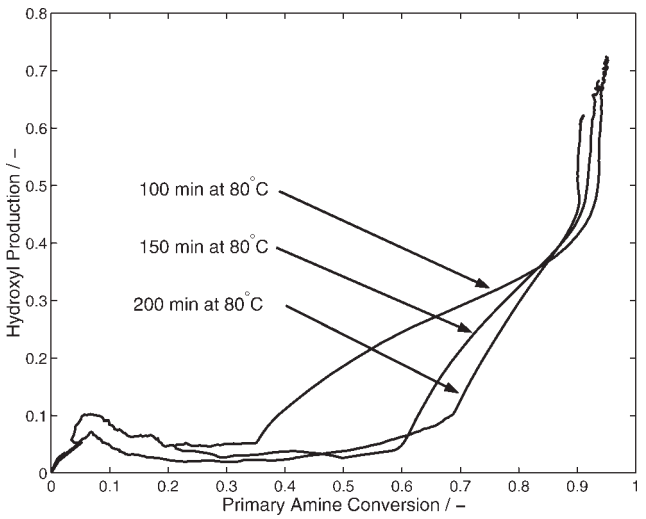

Figure 8 Production of hydroxyl initiated at 80°C as a function of the primary amine conversion, measured with NIR analysis.

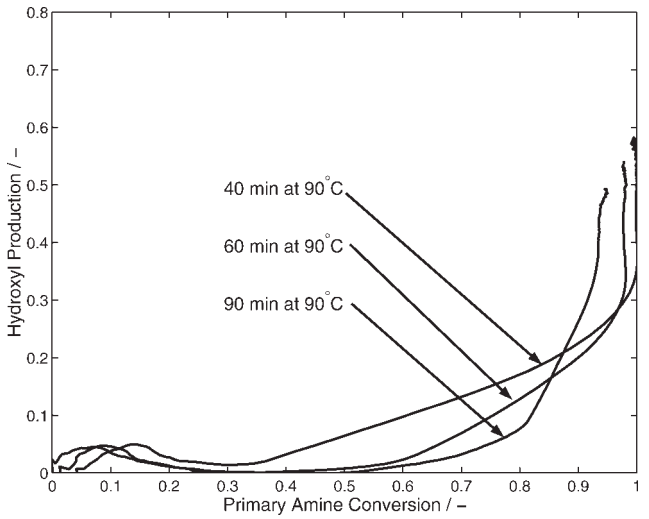

Figure 9 Production of hydroxyl initiated at 90°C as a function of the primary amine conversion, measured with NIR analysis.

tion of hydroxyl, but the conversion of primary amine would not be affected; this explains the smaller values of primary amine conversion. The effect could be caused by the low cure temperatures, which lead to a smaller amount of primary amine being incorporated into the epoxy network because of the poor solubility of DDA. This would leave small pockets of undissolved DDA, with which the epoxy is less prone to react. However, the primary amine that has been converted into a secondary amine is incorporated into the network structure and is able to react with the epoxy. Clearly, a more detailed study of the heterogeneity of the system with respect to undissolved DDA would be of significant interest.

Heat capacity measurements and MDSC

The dotted lines in Figures 10 and 11 indicate a short period of time in which no measurement of heat capacity was available because of transient effects originating from the DSC instrument during the change in temperature from 80 to 110°C. All measurements of heat capacity are relative because of problems with the calibration of heat capacity; however, the changes in heat capacity as a function of time would not be affected by these problems. The curves in Figures 10 and 11 are shifted in the y direction because of space limitations and to clarify the measured changes in the heat capacity. The scale is indicated by a vertical bar.

Mele et al.[53] and Regueira et al.[54] used the MDSC method to measure the heat capacity isothermally during reactions of epoxy, and Assche et al.[55] used the method to measure the heat capacity during reactions of unsaturated polyester resin with styrene. Curves similar to those in Figures 10 and 11 can be encountered in all three articles, in which the decrease in the heat capacity in the later stages of cure is attributed to vitrification. The point of inflection of the heat capacity curve is used to define vitrification according to refs. [54] and [55]. In Figures 10 and 11, vitrification occurs in the second part of the temperature program, that is, after the temperature has been increased to 110°C. Even for 200 min at 80°C and 90 min at 90°C, no vitrification was observed.

A small increase in the heat capacity was observed in the initial isothermal period for both 80 and 90°C before vitrification (see Figs. 10 and 11). These changes in the heat capacity were commented on by Assche et al.[55] for unsaturated polyester isothermal curing reactions, whereas Swier et al.[56] commented on changes in the heat capacity for epoxy resins. According to Swier et al. and references therein, the initial changes in the heat capacity are due to primary and secondary amine reactions. The primary amine–epoxy reactions give rise to positive variations in the heat capacity, whereas secondary amine–epoxy reactions give almost zero or even negative changes. This is consistent with Figures 6 and 7, in which a high degree of primary amine conversion is present in the initial isothermal curing period. An increase in the heat capacity would accordingly be expected.

A notable increase in the heat capacity was observed when the temperature was increased from moderate temperatures (80 or 90°C) to 110°C. Some part of this increase can be attributed to transient effects and to the temperature dependence of the heat capacity. An additional observation can be made in Figure 11 concerning the magnitude of the heat capacity change. The heat capacity increased approximately 0.06 J/g $^{\circ}C^{-1}$ for the experiment with 40 min at 90°C but only 0.025 J/g $^{\circ}C^{-1}$ for the experiment with 90 min at 90°C. A similar effect can be observed less clearly in Figure 10.

The more primary and secondary amine addition reactions there are at moderate temperatures, the fewer amine addition reactions there are at 110°C. Accordingly, the differences in the heat capacity for the cure cycle with 40 and 90 min at 90°C are explained by a larger number of primary amine addition reactions for the cure cycle with 90 min at 90°C. The increase in the heat capacity associated with primary amine addition reactions[57] will almost entirely occur in the 90°C period; hence, the increase in the heat capacity occurring in the 110°C period can be primarily attributed to a temperature dependence of the heat capacity.

One should also note that during the transient period in which the temperature is increased from 90 to 110°C, no heat capacity measurements are avail-

able. It is believed that in this short period, a large number of primary and secondary amine addition reactions occur (because of the increased temperature), explaining the large values of the heat capacity change for the cure cycles of 40 and 60 min at 90°C.

A comparison with Figure 7 shows that the primary amine conversion was approximately 0.8 just before the increase in temperature from 90 to 110°C for the 90 min at 90°C cure cycle. For the cure cycle with 40 min at 90°C, the primary amine conversion was approximately 0.3 just before the increase in temperature from 90 to 110°C. The 40-min cycle increased to a final primary amine conversion of approximately 1.0, and the 90-min cycle increased to a final primary amine conversion of approximately 0.95. Accordingly, for the 40-min cycle, the majority of the primary amine conversion was located in the 110°C period, and this also explains the large heat capacity increase for this cycle. For the 90-min cure cycle, the majority of the primary amine conversion was located in the 90°C period, and this explains the smaller heat capacity increase for this cycle. The primary amine conversion occurred very rapidly when the temperature was raised to 110°C, and this is consistent with the idea that a large number of primary and secondary amine addition reactions occur in the transition region in which no heat capacity measurements are available (marked with a dotted line in Figs. 10 and 11).

Swier et al.[57] found that the magnitude of the heat capacity difference at vitrification ($\Delta c_{p,\mathrm{Vit}}$), measured at the glass-transition temperature, increased with increasing conversion. In addition, the molar epoxy/amine ratio affected the magnitude of $\Delta c_{p,\mathrm{Vit}}$; hence, it increased to a maximum value when the molar epoxy/amine ratio equaled unity.

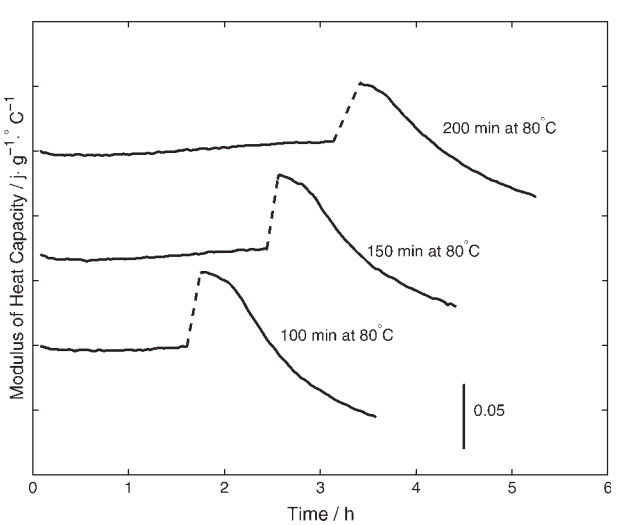

Figure 10 Heat capacity initiated at 80°C as a function of time, measured with MDSC. The dotted lines indicate a transient period for which no heat capacity data are available (see the text).

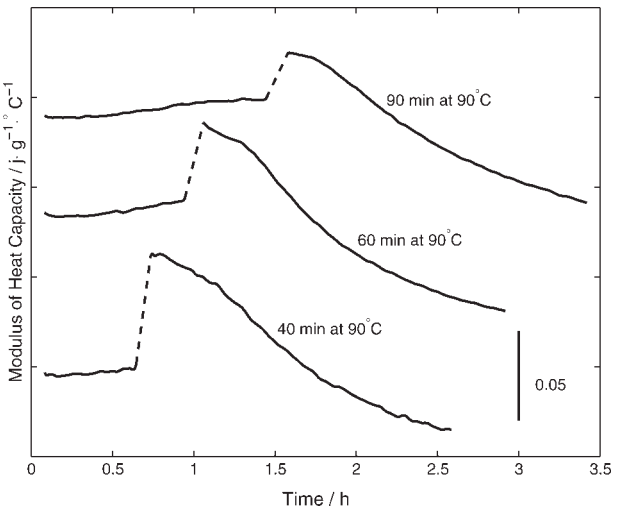

Figure 11 Heat capacity initiated at 90°C as a function of time, measured with MDSC. The dotted lines indicate a transient period for which no heat capacity data are available (see the text).

The notable decrease in the heat capacity during the later stages of cure (see Figs. 10 and 11) is attributed to vitrification, as mentioned previously. However, as the vitrification occurs over a broad range and does not seem to reach a stable value, the estimation of $\Delta c_{p,\mathrm{Vit}}$ is associated with some uncertainty. Generally, it seems that the magnitude of $\Delta c_{p,\mathrm{Vit}}$ increases with a decreasing curing time for periods at 80 or 90°C. Accordingly, the estimated values of $\Delta c_{p,\mathrm{Vit}}$ imply that the highest conversion rates are obtained in the short cure cycles, that is, 100 min at 80°C and 40 min at 90°C, and this is also confirmed by higher primary amine conversions and hydroxyl production, as illustrated in Figures 6–9.

This effect is thought to be caused by an increased number of etherification reactions at low temperatures, which leave less epoxy to participate in epoxy–amine addition reactions when the temperature is increased to 110°C. Accordingly, when the cure cycle is restricted to short periods at low temperatures, a larger amount of epoxy is available for epoxy–amine addition reactions when the temperature is increased to 110°C. This is also confirmed in Figures 6–9, in which the cure cycles with the shortest cure periods at 80 or 90°C also have the highest conversion of primary amine and the highest production of hydroxyl.

This information suggests that the mathematical modeling of the degree of cure obtained on the basis of isothermal DSC measurements may predict the same degree of cure, although different thermoset materials are obtained with different material properties.

CONCLUSIONS

The measurements of the degree of cure using DSC indicate lower values for cure cycles initiating at 80°C versus 90°C. The postcure treatment at 110°C would ideally make the epoxy system approach an almost complete cure, which, however, was not achieved for cure cycles initiating at 80°C. This effect is attributed to different reaction mechanisms for cure cycles initiating at 80 and 90°C.

A mathematical model was constructed to predict the degree of cure under different cure cycles. The model is based on isothermal DSC measurements and approaches the maximum possible degree of cure at a certain temperature without respect to the previous cure cycles. This will inherently lead to problems with cure cycles initiating at 80°C. Accordingly, large discrepancies were observed between the measured and predicted degrees of cure for all cure cycles initiating at 80°C; however, for all cure cycles initiating at 90°C, only small discrepancies existed. If a more accurate mathematical model is required, a detailed mass balance must be made, which, however, is difficult because the reaction mechanisms are not known in detail. Clearly, using the applied mathematical model for predicative purposes would be associated with some degree of error.

The NIR analysis indicated almost 100% epoxy conversion for all cure cycles. The primary amine conversion increased with decreasing time at low temperatures and was consistent with hydroxyl production; the highest hydroxyl production also was highest for cure cycles with the shortest time at a low temperature, that is, 100 min at 80°C and 40 min at 90°C. These observations indicate that etherification is more likely to occur at a low temperature than epoxy–amine addition; hence, a lower amount of primary amine is incorporated into the epoxy network during curing at low temperatures for prolonged periods (i.e., 200 min at 80°C and 90 min at 90°C), and this results in lower hydroxyl production.

The primary amine conversions for cure cycles initiated at 80°C were generally found to be less than those for cure cycles initiated at 90°C. However, the largest hydroxyl production was found for cure cycles initiated at 80°C, and this at first seems to be inconsistent with the lower primary amine conversion. These findings are supposedly caused by a substitution effect in which the epoxy is more likely to react with secondary amine than primary amine. This would lead to a continued conversion of epoxy and production of hydroxyl, but the conversion of primary amine would not be affected; this could explain the smaller values of primary amine conversion. The substitution effect could be caused by the low cure temperatures, which lead to a smaller amount of primary amine being incorporated into the epoxy network because of the poor solubility of DDA. This would leave small pockets of undissolved primary amine, with which the epoxy is less prone to react. However, the primary amine that has reacted is incorporated into the network structure and is closely connected to a secondary amine, with which the epoxy is more prone to react.

MDSC measurements revealed small increases in the heat capacity in the initial curing period indicating primary amine conversion. An increase in the heat capacity occurred when the temperature was increased from either 80 or 90°C to 110°C. This effect is primarily attributed to a positive temperature dependence of the heat capacity. In addition, the heat capacity change was larger after short curing periods at low temperatures, and this indicated that a relatively large amount of primary amine conversion occurred during the transient period in which the temperature was increased from 80 or 90°C to 110°C. The primary amine conversion, measured by NIR analysis, confirmed the behavior; that is, a large primary amine conversion was observed during and just after the transient period for the short cure cycles, thereby increasing the heat capacity.

MDSC measurements indicated vitrification in the postcure treatment at 110°C for all six cure cycles. The onset of vitrification was observed not in any of the cure cycles at 80 or 90°C but only in the postcure treatment period at 110°C. The magnitude of $\Delta c_{p,\mathrm{Vit}}$ increased with decreasing curing time at 80 or 90°C, implying that the highest conversion rates were obtained in the short cure cycles, that is, 100 min at 80°C and 40 min at 90°C. This was also confirmed by a higher primary amine conversion and hydroxyl production.

The authors thank technicians Carsten Andreasen, Jens Erik Nielsen, Henry Enevoldsen, Per Friis Nielsen, and Jens Hedevang Christensen for assistance with instrumentation, electrical systems, mechanical tool work, and three-dimensional illustrations. They also kindly thank Milosz Adam Gwizdalski for the many DSC analyses performed. They also kindly thank the anonymous referees for their helpful comments.

References

1. Ellis, B. Chemistry and Technology of Epoxy Resins; Blackie: London, 1993.
2. Zahir, S. A. Adv Org Coat Sci Technol 1983, 4, 83.
3. Saunders, T. F.; Levy, M. F.; Serino, J. F. J Polym Sci 1967, 5, 1609.
4. Gilbert, M. D.; Schneider, N. S.; MacKnight, W. J. Macromolecules 1991, 24, 360.
5. Schneider, N. S.; Sprouse, J. F.; Hagnauer, G. L.; Gillham, J. K. Polym Eng Sci 1979, 19, 304.
6. Eyerer, P. J Appl Polym Sci 1971, 15, 3067.

7. Eyerer, P. Polymer 1973, 14, 91.
8. Hong, S.-G.; Wu, C.-S. Thermochim Acta 1998, 316, 167.
9. Son, P.-N.; Weber, C. D. J Appl Polym Sci 1973, 17, 1305.
10. Fedtke, M.; Domaratius, F.; Pfitzmann, A. Polym Bull 1990, 23, 381.
11. Pfitzmann, A.; Fliedner, E.; Fedtke, M. Polym Bull 1994, 32, 311.
12. Pfitzmann, A.; Sclothauer, K.; Fedtke, M. Polym Bull 1991, 27, 59.
13. Poisson, N.; Maazouz, A.; Sautereau, H.; Taha, M.; Gambert, X. J Appl Polym Sci 1998, 69, 2487.
14. Poisson, N.; Lachenal, G.; Sautereau, H. Vibr Spectrosc 1996, 12, 237.
15. Pfitzmann, A.; Fedtke, M. Kautsch Gummi Kunstst 1993, 46, 596.
16. Barwich, J.; Guse, D.; Brockmann, H. Adhesion 1989, 5, 27.
17. Wang, Q.; Storm, B. K.; Houmøller, L. P. J Appl Polym Sci 2003, 87, 2295.
18. Gundjian, M.; Cole, K. C. J Appl Polym Sci 2000, 75, 1458.
19. Lin, Y. G.; Galy, J.; Sautereau, H.; Pascault, J. P. In Crosslinked Epoxies: Proceedings of the 9th Discussion Conference, Prague, Czechoslovakia, July 14–17, 1986; Sedlàcek, B., Ed.; de Gruyter: Berlin, 1987.
20. Güthner, T.; Hammer, B. J Appl Polym Sci 1993, 50, 1453.
21. Barton, J. M. Adv Polym Sci 1985, 72, 111.
22. Lin, Y. G.; Sautereau, H.; Pascault, J. P. J Appl Polym Sci 1986, 32, 4595.
23. Amdouni, N.; Sautereau, H.; Gérard, J. F.; Pascault, J. P. J Appl Polym Sci 1990, 31, 1245.
24. Oleinik, E. F. Epoxy Resins and Composites IV; Springer-Verlag: Berlin, 1986.
25. Barral, L.; Cano, J.; López, J.; López-Bueno, I.; Nogueira, P.; Ramirez, C.; Torres, A.; Abad, M. J. J Therm Anal Calorim 1999, 56, 1025.
26. Barral, L.; Cano, J.; López, J.; López-Bueno, I.; Nogueira, P.; Abad, M. J.; Torres, A.; Ramirez, C. J Appl Polym Sci 2000, 77, 2305.
27. Vergnaud, J.-M.; Bouzon, J. Cure of Thermosetting Resins: Modelling and Experiments; Springer-Verlag: Berlin, 1992.
28. Hale, A. In Handbook of Thermal Analysis and Calorimetry; Cheng, S. Z. D., Ed.; Elsevier: Amsterdam, 2002; Chapter 9.
29. Höhne, G.; Hemminger, W.; Flammersheim, H.-J. Differential Scanning Calorimetry: An Introduction for Practitioners, 2nd ed.; Springer-Verlag: Berlin, 1996.
30. Richardson, M. J. In Calorimetry and Thermal Analysis of Polymers, Mathot, V. B. F., Ed.; Hanser: Munich, 1993; Chapter 7.
31. Keenan, M. R. J Appl Polym Sci 1987, 33, 1725.
32. Sourour, S.; Kamal, M. R. Thermochim Acta 1976, 14, 41.
33. Kosar, V.; Gomzi, Z. Chem Biochem Eng Q 2001, 15, 101.
34. Ryan, M. E.; Dutta, A. Polymer 1979, 20, 203.
35. Lee, J. Y.; Choi, H. K.; Shim, M. J.; Kim, S. W. Thermochim Acta 2000, 343, 111.
36. Crosby, P. A.; Powell, G. R.; Fernando, G. F.; France, C. M.; Spooncer, R. C.; Waters, D. N. Smart Mater Struct 1996, 5, 415.
37. Yi, S.; Hilton, H. H.; Ahmed, M. F. Comput Struct 1997, 64, 383.
38. Hayes, B. S.; Gilbert, E. N.; et al. Presented at the 31st International SAMPE Technical Conference, Chicago, Illinois, Oct 26–30, 1999.
39. Rice, B. P.; Lee, C. W.; et al. Presented at the 45th International SAMPE Symposium, Long Beach, California, May 21–25, 2000.
40. Flach, L.; Bryant, E.; et al. Presented at the 45th International SAMPE Symposium, Long Beach, California, May 21–25, 2000.
41. Ng, S. J.; Boswell, R.; et al. Presented at the 45th International SAMPE Symposium, Long Beach, California, May 21–25, 2000.
42. Nelson, K. M.; Poursartip, A.; Fernlund, G. Presented at the 45th International SAMPE Symposium, Long Beach, California, May 21–25, 2000.
43. Lee, K.; Biney, P. O.; Zhong, Y. Presented at the 46th International SAMPE Symposium, Long Beach, California, May 6–10, 2001.
44. Yang, H.; Lee, L. J. Presented at the 31st International SAMPE Technical Conference, Chicago, Illinois, Oct 26–30, 1999.
45. Yang, F.; Pitchumani, R. Presented at the 49th International SAMPE Symposium, Long Beach, California, May 16–20, 2004.
46. Guo, Z.-S.; Du, S.; Zhang, B. Presented at the 49th International SAMPE Symposium, Long Beach, California, May 16–20, 2004.
47. Rasekh, A.; Vaziri, R.; Poursartip, A. Presented at the 36th International SAMPE Technical Conference, San Diego, California, Nov 15–18, 2004.
48. Guo, Z.-S.; Du, S.-Y.; et al. Presented at the 35th International SAMPE Technical Conference, Dayton, Ohio, Sept 28 to Oct 2, 2003.
49. Guo, Z.-S.; Du, S.-Y.; et al. Presented at the 35th International SAMPE Technical Conference, Dayton, Ohio, Sept 28 to Oct 2, 2003.
50. Johnston, A.; Palmese, G.; et al. Presented at the 35th International SAMPE Technical Conference, Dayton, Ohio, Sept 28 to Oct 2, 2003.
51. Garcia-Padron, R.; Kenny, J. M.; Berglund, L. A. Modeling the Processing Behaviour of Epoxy Composite Laminates; Licentiate Theses 341; Institute of Technology: Linköping, Sweden, 1992.
52. Kissinger, H. E. Anal Chem 1957, 29, 1702.
53. Mele, B. V.; Assche, G. V.; Hemelrijck, A. V. J Reinforced Plast Compos 1999, 18, 885.
54. Regueira, L. N.; Barreiro, S. G.; Frenandez, C. A. G. J Therm Anal Calorim 2005, 82, 797.
55. Assche, G. V.; Verdonck, E.; Mele, B. V. Polymer 2001, 42, 2959.
56. Swier, S.; Van Assche, G.; Van Hemelrijck, A.; Rahier, H.; Verdonck, E.; Mele, B. V. J Therm Anal 1998, 54, 585.